ACKNOWLEDGMENT

The authors thank the mobility program of the Vicerrectorado de Investigación of Carlos III University of Madrid for the help supplied. Also, they want to thank C. J. Sánchez-Fernández for manufacturing the prototypes.

REFERENCES

[1] C. Martín-Pascual, E. Rajo-Iglesias, and V. González-Posadas, "Invited tutorial: Patches: The most versatile radiator?," presented at the IASTED Int. Conf. Adv. Commun., Jul. 2001.

[2] J. R. James and P. S. Hall, *Handbook of Microstrip and Printed Antennas*. New York: Wiley, 1997.

[3] C. Balanis, *Antenna Theory: Analysis and Design*. Hoboken, NJ: Wiley Interscience, 2005.

[4] S. Maci and G. Gentili, "Dual-frequency patch antennas," *IEEE Antennas Propag. Mag.*, vol. 39, no. 6, pp. 13–20, Dec. 1997.

[5] E. Rajo-Iglesias, O. Quevedo-Teruel, and L. Inclan-Sanchez, "Mutual coupling reduction in patch antenna arrays by using a planar EBG structure and a multilayer dielectric substrate," *IEEE Trans. Antennas Propag.*, vol. 56, no. 6, pp. 1648–1655, Jun. 2008.

[6] J. Robinson and Y. Rahmat-Samii, "Particle swarm optimization in electromagnetics," *IEEE Trans. Antennas Propag.*, vol. 52, no. 2, pp. 397–407, Feb. 2004.

[7] S. Long and M. Walton, "A dual-frequency stacked circular-disc antenna," *IEEE Trans. Antennas Propag.*, vol. AP-27, no. 2, pp. 270–273, Mar. 1979.

[8] R. Q. Lee, K. F. Lee, and J. Bobinchak, "Characteristics of a two-layer electromagnetically coupled rectangular patch antenna," *Electron. Lett.*, vol. 23, pp. 1070–1072, Sep. 1987.

[9] E. Rajo-Iglesias, G. Villaseca-Sánchez, and C. Martín-Pascual, "Input impedance behavior in offset stacked patches," *IEEE Antennas Wireless Propag. Lett.*, vol. 1, pp. 28–30, Jan. 2002.

[10] R. Waterhouse, "Stacked patches using high and low dielectric constant material combinations," *IEEE Trans. Antennas Propag.*, vol. 47, pp. 1767–1771, Dec. 1999.

[11] A. Panther, A. Petosa, M. Stubbs, and K. Kautio, "A wideband array of stacked patch antennas using embedded air cavities in LTCC," *IEEE Microw. Wireless Compon. Lett.*, vol. 15, no. 12, pp. 916–918, Dec. 2005.

[12] C. Terret, S. Assailly, K. Mahdjoubi, and M. Edimo, "Mutual coupling between stacked square microstrip antennas fed on their diagonal," *IEEE Trans. Antennas Propag.*, vol. 39, pp. 1049–1051, Jul. 1991.

[13] R. Zentner, Z. Sipus, and J. Bartolic, "Theoretical and experimental study of mutual coupling between microstrip stacked patch antennas," in *Proc. IEEE Antennas Propagation Soc. Int. Symp.*, Jun. 2003, vol. 1, pp. 618–621, vol. 1.

[14] K. Chung and A. Mohan, "Mutual coupling between stacked CP-EMCP antennas," in *Proc. IEEE Antennas Propagation Soc. Int. Symp.*, Jul. 2005, vol. 2A, pp. 246–249, vol. 2A.

[15] R. Q. Lee and K. F. Lee, "Experimental study of the two-layer electromagnetically coupled rectangular patch antenna," *IEEE Trans. Antennas Propag.*, vol. 38, pp. 1298–1302, Aug. 1990.

[16] Z. Sipus, P.-S. Kildal, R. Leijon, and M. Johansson, "An algorithm for calculating Green's functions for planar, circular cylindrical and spherical multilayer substrates," *Appl. Computat. Electromagn. Soc. J.*, vol. 13, pp. 243–254, Nov. 1998.

[17] N. Herscovici, Z. Sipus, and D. Bonefacic, "Circularly polarized single-fed wide-band microstrip patch," *IEEE Trans. Antennas Propag.*, vol. 51, pp. 1277–1280, Jun. 2003.

Synthesis and Design of a New Printed Filtering Antenna

Chao-Tang Chuang and Shyh-Jong Chung

***Abstract*—Synthesis and design of a new printed filtering antenna is presented in this communication. For the requirements of efficient integration and simple fabrication, the co-design approach for the integration of filter and antenna is introduced. The printed inverted-L antenna and the parallel coupled microstrip line sections are used for example to illustrate the synthesis of a bandpass filtering antenna. The equivalent circuit model for the inverted-L antenna, which is mainly a series RLC circuit, is first established. The values of the corresponding circuit components are then extracted by comparing with the full-wave simulation results. The inverted-L antenna here performs not only a radiator but also the last resonator of the bandpass filter. A design procedure is given, which clearly indicates the steps from the filter specifications to the implementation. As an example, a 2.45 GHz third-order Chebyshev bandpass filter with 0.1 dB equal-ripple response is tackled. Without suffering more circuit area, the proposed structure provides good design accuracy and filter skirt selectivity as compared to the filter simple cascade with antenna and a bandpass filter of the same order. The measured results, including the return loss, total radiated power, and radiation gain versus frequency, agree well with the designed ones.**

***Index Terms*—Chebyshev bandpass filter, filtering antenna, filter synthesis, inverted-L antenna, skirt selectivity.**

I. INTRODUCTION

In many wireless communication systems, the RF filters are usually placed right after the antenna. Since the size reduction and low profile structure are a trend in the circuit design, it is desired to integrate the bandpass filter and antenna in a single module, so called *filtering antenna*, with filtering and radiating functions simultaneously. However, to date, there has been relatively little research conducted on an efficient integration between the filter and antenna with simple fabrication and good circuit behavior. In traditional design, the filter and the antenna are designed individually, with the common ports' characteristic impedance Z_0, and then connected directly. The direct connection of the filter and antenna usually causes an impedance mismatch, which may deteriorate the filter's performance (especially near the band edges) and increase the insertion loss of the circuitry. To avoid this, extra matching network should be implemented in between these two components [1].

Several investigations have been focused on adding the radiating or filtering function into an antenna or filter [2], [3]. In [2], metal posts were inserted into a horn antenna, which can generate the filtering function. And in [3], the way is to create coupled cavities into a leaky wave antenna so as to generate filtering performance on the antenna. While these proposed circuits possess the characteristics of filtering and radiating, it should be noted that they were designed without using a systematic approach nor considering much on the filter's or antenna's specifications.

Various approaches for integrating the filter and antenna into a single microwave device have been discussed in [4], [5]. For size reduction, a

Manuscript received July 20, 2009; revised July 07, 2010; accepted November 02, 2010. Date of publication January 06, 2011; date of current version March 02, 2011. This work was supported in part by the National Science Council, R.O.C., under Contract NSC 97-2221-E-009-041-MY3.

The authors are with the Institute of Communication Engineering, National Chiao Tung University, Hsinchu, Taiwan 30050, R.O.C (e-mail: sjchung@cm.nctu.edu.tw).

Color versions of one or more of the figures in this communication are available online at http://ieeexplore.ieee.org.

Digital Object Identifier 10.1109/TAP.2010.2103001

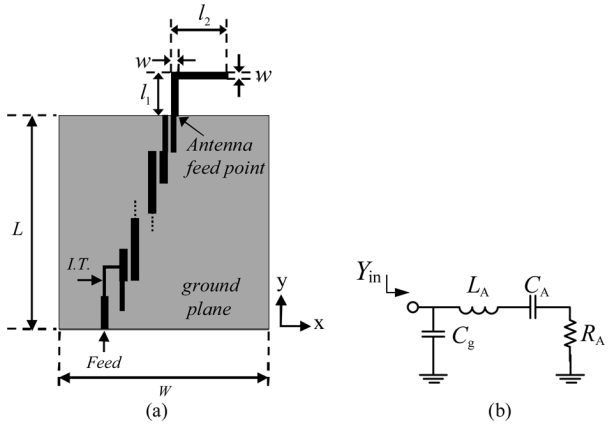

Fig. 1. (a) Configuration of the proposed filtering antenna. (b) the equivalent circuit of the inverted-L antenna. ($\mathrm{I.T.} = \mathrm{ImpedanceTransformer}$).

pre-designed bandpass filter with suitable configuration was directly inserted into the feed position of a patch antenna [4]. By using an extra impedance transformation structure in between the filter and the antenna, the bandpass filter can be integrated properly with the antenna over the required bandwidth [5]. However, the transition structure needs additional circuit area, and the designs did not have good filter characteristics over the frequency range.

Recently, several filtering antennas designed following the synthesis process of the bandpass filter have been presented [6], [7]. In these designs, the last resonator and the load impedance of the bandpass filter were substituted by an antenna that exhibited a series or parallel RLC equivalent circuit. Although they have been done based on the co-design approach, most of them did not show good filter performance, especially the band-edge selectivity and stopband suppression. This is due to the lack of the extraction of the antenna's equivalent circuit over a suitable bandwidth. Only that at the center frequency was extracted and used in the filter synthesis. Moreover, the antenna gain versus frequency, which is an important characteristic of the filtering antenna, was not examined in these studies. Although in [7], the frequency response of a factor named *ideal matching loss* ($= 1 - |\mathrm{S}_{11}|^2$) was considered, it did not take into account the circuit and antenna losses and thus missed the power transmission characteristic of the filtering antenna.

In this study, a new co-design method is proposed to achieve a filtering antenna with printed structure as shown in Fig. 1(a), which contains an inverted-L antenna and $N-1$ parallel half-wavelength microstrip lines. The printed inverted-L antenna is used with its equivalent circuit completely extracted over a desired bandwidth for the synthesis of the filtering antenna. Also, to increase the fabrication tolerance, a quarter-wave admittance inverter with characteristic impedance other than Z_0 is introduced in the filter synthesis.

II. Equivalent Circuit Model of The Inverted-L Antenna

Since the antenna is to be designed in the filter as the last resonator, the first step to synthesize the filtering antenna is to establish the antenna's equivalent circuit model and extract the circuit components. Fig. 1(b) shows the equivalent circuit at the antenna feed point looking toward the antenna. Since the inverted-L antenna is a variety of a monopole antenna, the antenna exhibits a series RLC resonance near the first resonant frequency [8]. Here, L_A and C_A express the resonant inductance and capacitance of the antenna, respectively, and R_A corresponds to the antenna radiation resistance. It is noted that an extra shunt capacitance C_g is incorporated in the equivalent circuit here so that, as will be seen below, the whole circuit would have the same impedance behavior as the antenna itself in a wider frequency range. This parasitic capacitance comes from the accumulation of charges around the antenna feed point due to the truncation of the ground plane.

The inverted-L antenna is printed on a 0.508 mm Rogers 4003 substrate with a dielectric constant of 3.38 and loss tangent of 0.0027. The ground plane of the antenna, which is also the ground plane of the circuitry, has a fixed size of $L \times W = 60\ \mathrm{mm} \times 60\ \mathrm{mm}$. The antenna is fed through a 50 Ω microstrip line of width 1.17 mm. In the following, the simulated characteristics of all the structures (filters and antennas) are performed by the full-wave simulator Ansoft HFSS (High Frequency Structure Simulator based on the finite element method), while those of the antenna's equivalent circuit are by AWR MWO (Microwave Office). For each given inverted-L antenna structure, the equivalent circuit components are extracted by first letting the resonant frequency of the circuit equal the simulated resonant frequency of the antenna. And then, we optimize the values of the circuit components so that the reflection coefficient (S_{11}), as a function of frequency, of the equivalent circuit coincides with that simulated from the antenna in a frequency range as wide as possible. The difference $\Delta\mathrm{S}_{11}$ of the reflection coefficient between these two curves is set not beyond 3% in a 20% frequency bandwidth centered at the antenna resonant frequency.

In this design, the radiation resistance R_A in the equivalent circuit can serve as the load impedance of the bandpass filter to be synthesized, and the series L_A-C_A circuit can be the filter's last resonator so that

$$f_0 = \frac{1}{2\pi\sqrt{L_\mathrm{A}C_\mathrm{A}}} \tag{1}$$

where f_0 is the center frequency of the bandpass filter and is chosen as 2.45 GHz in this work. In the process of establishing the antenna database, the antenna frequency f_A, which is determined by the total strip lengths ($l_1 + l_2 \approx \lambda_\mathrm{A}/4$), should be slightly larger than f_0 due to the existence of the parasitic capacitance C_g. This frequency corresponds to the frequency location of the minimum value of the antenna's reflection coefficient (S_{11})

$$\mathrm{S}_{11} = 20\log\left|\frac{Y_\mathrm{in} - Y_0}{Y_\mathrm{in} + Y_0}\right| \tag{2}$$

with

$$Y_\mathrm{in} = j2\pi f C_\mathrm{g} + \left[R_\mathrm{A} + j2\pi f L_\mathrm{A}\left(1 - \frac{f_0^2}{f^2}\right)\right]^{-1}.$$

It is noted that the radiation resistance R_A and the inductance L_A are mainly dependent on the vertical strip length l_1 due to the strongest current distribution on this strip. Also, the parasitic capacitance C_g is decided by the strip width w and independent of the strip length l_1. It is thus observed that the values of the three components ($R_\mathrm{A}, L_\mathrm{A}, C_\mathrm{g}$) in (2) are almost invariant at a fixed strip length l_1 only if the antenna frequency is near f_0. Therefore, for a choosing strip length, we first extract the components of the $R_\mathrm{A}, L_\mathrm{A}$, and C_g when the antenna is resonated at f_0, and then, taking these three components into (2), the resonant frequency f_A can be obtained. Various values of l_1 have been analyzed in this study. It is found out that, the antenna with different dimensions of l_1 has the resonant frequency f_A near 2.53 GHz while f_0 is 2.45 GHz.

Another important factor to be used for synthesizing the filtering antenna is the corresponding quality factor of the antenna, Q_A, which is defined as

$$Q_\mathrm{A} = \frac{2\pi f_0 L_\mathrm{A}}{R_\mathrm{A}} \tag{3}$$

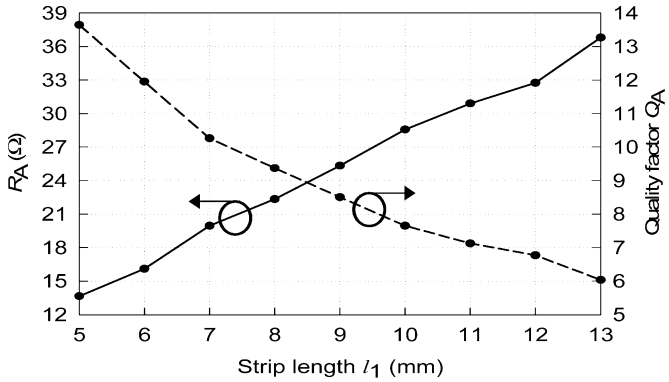

Fig. 2. The radiation resistance $R_{\rm A}$ and quality factor $Q_{\rm A}$ as a function of the strip length l_1. $w = 1.17$ mm, $f_0 = 2.45$ GHz.

and is that of the series RLC circuit in the antenna's equivalent circuit, without including the effect of the parasitic capacitance $C_{\rm g}$. It should be noticed that the $Q_{\rm A}$ is not the whole quality factor of the inverted-L antenna.

Fig. 2 shows the variation of the radiation resistance $R_{\rm A}$ and quality factor $Q_{\rm A}$ as a function of the strip length l_1. It can be observed that the radiation resistance $R_{\rm A}$ increases substantially from 13.6 Ω to 36.8 Ω when the strip length l_1 changes from 5 mm to 13 mm. In the same l_1 variation range, the inductance $L_{\rm A}$ (not shown in the figure) has only little change (from 12 nH to 14.5 nH). The radiation resistance increases much fast than the inductance as the strip length increases, which results in a decreasing quality factor due to (3). As seen, the quality factor changes from 13.7 to 6.0 when l_1 increases from 5 mm to 13 mm. Although not shown here, the strip width w has minor influence on the values of equivalent circuit components. And the extracted parasitic capacitance $C_{\rm g}$ is around 0.3 pF to 0.4 pF, roughly independent of the variations of l_1 and w. As to the application in the synthesis of the proposed filtering antenna, once the quality factor $Q_{\rm A}$ is determined by the given specifications of filter (the relationship will be derived later), the values of l_1 and $R_{\rm A}$ can be obtained via the $Q_{\rm A}$ -to-l_1 and $R_{\rm A}$-to-l_1 curves in Fig. 2, respectively, and then the dimensions of the antenna can be obtained.

Fig. 3 shows the comparison of the impedance behaviors on the Smith chart from the full-wave simulation and the equivalent circuit calculation. The dimensions of the inverted-L antenna, which is to be used later in the synthesis of the filtering antenna, are $l_1 = 10$ mm, $w = 1.17$ mm, and $l_2 = 17.25$ mm. The extracted circuit components are $L_{\rm A} = 14.2$ nH, $C_{\rm A} = 0.30$ pF, $R_{\rm A} = 28.6\ \Omega$, and $C_{\rm g} = 0.37$ pF, with the corresponding quality factor $\rm Q_A = 7.65$. Notice that $C_{\rm g}$ has the same level as $C_{\rm A}$ so that this parasitic capacitance can not be neglected in the modeling of the antenna. It is seen from the figure that the curve of $\rm S_{11}$ for the equivalent circuit agrees well with the full-wave simulation one from 1.5 GHz to 4 GHz. Especially, they have the same value at the antenna resonant frequency ($f_{\rm A} = 2.53$ GHz), and the difference $\Delta \rm S_{11}$ is 0.16 dB (error of $\Delta \rm S_{11} \approx 3\%$) at $f = 2.28$ GHz and 0.148 dB (error of $\Delta \rm S_{11} \approx 3\%$) at $f = 2.81$ GHz.

III. Synthesis of the Filtering Antenna

Fig. 4(a) shows the proposed filtering antenna, which contains N coupled line sections and an inverted-L antenna. Note that the antenna is connected directly to the Nth coupled line. The filter to be synthesized is an Nth order Chebyshev bandpass filter. The $N-1$ filter resonators are provided by the coupled line sections and the last one by the inverted-L antenna. In order to match to the low antenna radiation resistance and increase the flexibility of design, here the Nth coupled line

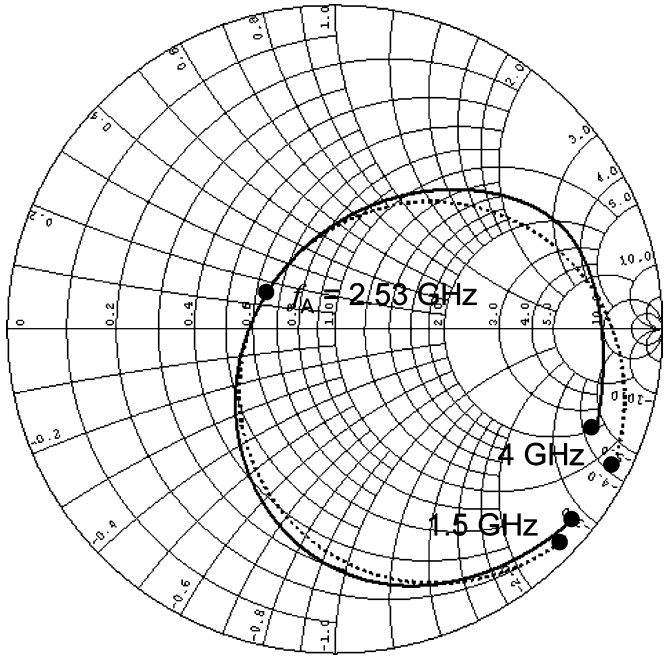

Fig. 3. Input impedances of the inverted-L antenna with $l_1 = 10$ mm, $w = 1.17$ mm, and $l_2 = 17.25$ mm. (solid line: the full-wave simulation; dotted line: the equivalent circuit calculation.

has different design as the conventional ones [9]. Consider a coupled line section with even- and odd-mode characteristic impedances $Z'_{\rm 0eN}$ and $Z'_{\rm 0oN}$, respectively, as shown in Fig. 5(a), which is to be equivalent to the circuit shown in Fig. 5(b) near the center frequency f_0. The right transmission line section in Fig. 5(b) has a characteristic impedance $Z_{\rm a}$, which is different from the system impedance $Z_0 (= 50\ \Omega)$ and can be selected arbitrarily. To have the same circuit performances near the center frequency, the ABCD matrices of the coupled line section and the equivalent circuit should be equal at $\theta' = \pi/2$, resulting into

$$Z'_{\rm 0eN} = Z_{\rm a}[Z_0/Z_{\rm a} + J'_{\rm N} Z_0 + (J'_{\rm N} Z_0)^2] \tag{4a}$$

$$Z'_{\rm 0oN} = Z_{\rm a}[Z_0/Z_{\rm a} - J'_{\rm N} Z_0 + (J'_{\rm N} Z_0)^2]. \tag{4b}$$

Therefore, once $J'_{\rm N} Z_0$ is known, the impedances and thus the dimensions of the Nth coupled line section can be obtained.

By using the equivalent circuits of the antenna and the coupled line sections, the filtering antenna structure shown in Fig. 4(a) can be expressed by the equivalent circuit shown in Fig. 4(b). The two transmission line sections in between the admittance inverters have lengths equal to a half wavelength near the center frequency, i.e., $2\theta \approx \theta + \theta' \approx \pi$, and thus can be replaced by a parallel *LC* resonator as shown in the upper sub-figure of Fig. 4(c). To transfer this circuit to a typical bandpass filter topology, the antenna's parasitic capacitance $C_{\rm g}$ should be moved to the left-hand side of the admittance inverter $J'_{\rm N}$ as illustrated in Block 2 of Fig. 4(c). The resultant capacitance $C'_{\rm g}$ can be derived by equalizing the input admittances of Blocks 1 and 2 in the figure. For frequencies near f_0 and $\theta' \approx \pi/2$, the input admittance $Y^1_{\rm in}$ of Block 1 and $Y^2_{\rm in}$ of Block 2 can be derived and approximated as

$$Y^1_{\rm in} \approx J'^2_{\rm N} Z^2_{\rm a} \left(j2\pi f C_{\rm g} + \frac{1}{j\sqrt{\frac{L_{\rm A}}{C_{\rm A}}\left(\frac{f}{f_0} - \frac{f_0}{f}\right)} + R_{\rm A}} \right) \tag{5}$$

$$Y^2_{\rm in} = j2\pi f C'_g + Y'_{\rm in} \tag{6}$$

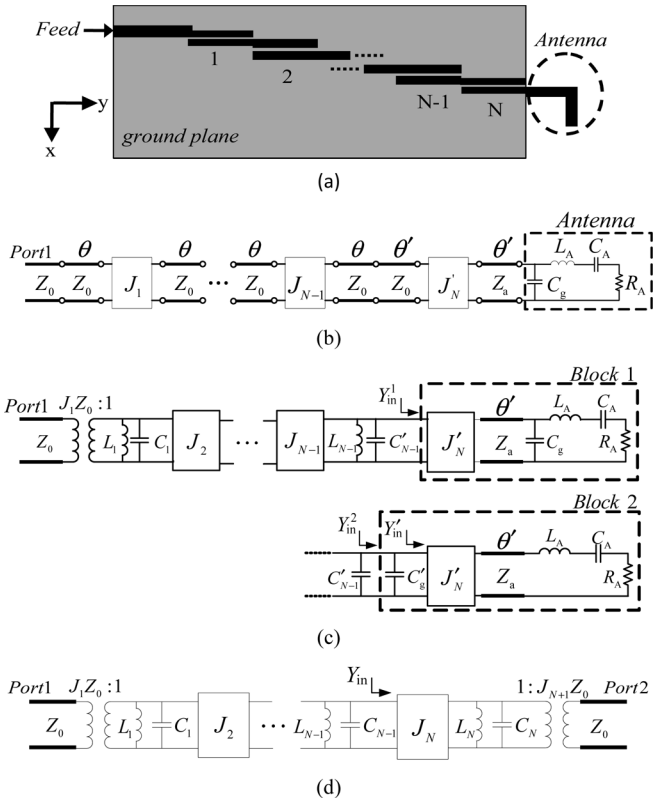

Fig. 4. (a) The structure of the proposed N-order filtering antenna. (b) Equivalent circuit of the proposed filtering antenna. (c) Modified circuit of the proposed filtering antenna. (d) A typical N-order bandpass filter circuit using shunt resonators with admittance inverters.

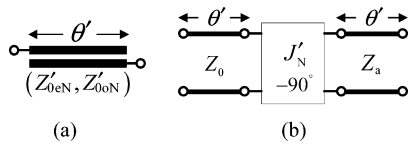

Fig. 5. (a) Geometry of the Nth coupled line section and (b) the corresponding equivalent circuit.

with

$$Y'_{\rm in} \approx \frac{J'^2_{\rm N} Z_{\rm a}^2}{j\sqrt{\frac{L_{\rm A}}{C_{\rm A}}}\left(\frac{f}{f_0}-\frac{f_0}{f}\right)+R_{\rm A}}. \tag{7}$$

By equalizing (5) and (6), one obtains

$$C'_{\rm g} = (J'_{\rm N} Z_{\rm a})^2 C_{\rm g}. \tag{8}$$

Actually, the capacitance $C'_{\rm g}$ is much smaller than $C'_{\rm N-1}$, therefore, the total capacitance $C_{N-1}(=C'_{\rm N-1}+C'_{\rm g})$ of the second resonator is approximately equal to $C'_{\rm N-1}$.

Finally, the equivalent circuit of Fig. 4(c) can be transferred to the conventional Nth order bandpass filter circuit as shown in Fig. 4(d), and, by letting the admittance $Y'_{\rm in}$ equal $Y_{\rm in}$, one obtains

$$Q_{\rm A} = \frac{2\pi f_0 L_{\rm A}}{R_{\rm A}} = \frac{\pi}{2(Z_0 J_{\rm N+1})^2} \tag{9}$$

and

$$J'_{\rm N} Z_0 = \frac{J_{\rm N} Z_0}{Z_{\rm a}}\left(\frac{2Q_{\rm A} R_{\rm A} Z_0}{\pi}\right)^{1/2}. \tag{10}$$

The design procedures of the proposed filtering antenna can now be summarized as follows.

1) Specify the requirements of the bandpass filter to be synthesized, including the center frequency f_0, the fractional bandwidth Δ, and the type of the filter (e.g., bandpass filter with equal ripple), from which the admittance inverters $J_{\rm n} Z_0 (n = 1, 2, \ldots, N+1)$ and the parallel resonators $L_n, C_{\rm n} (n = 1, 2, \ldots, N)$ in Fig. 4(d) can be determined [9].
2) Choose an antenna structure with suitable equivalent circuit that can substitute for the last resonator and load impedance of the bandpass filter. (Here in this study, the inverted-L antenna is used.) And then get a database associated with the equivalent circuit components for different antenna dimensions like those in Section II.
3) Calculate the antenna quality factor $Q_{\rm A}$ from (9) and then, after choosing a suitable strip width (e.g., the same width as the feed line), obtain the required strip length l_1 and radiation resistance $R_{\rm A}$ of the inverted-L antenna by using Fig. 2. The length l_2 of the horizontal antenna strip can thus be determined by letting the antenna resonate at $f_{\rm A}$. At this step, the dimensions of the inverted-L antenna are acquired.
4) Choose suitable characteristic impedance $Z_{\rm a}$ and then calculate the inverter constant $J'_{\rm N} Z_0$ by using (10). Following, the even- and odd-mode characteristic impedances $Z'_{\rm 0eN}$ and $Z'_{\rm 0oN}$ of the Nth coupled line section for the proposed filtering antenna can be attained via (4).
5) Calculate the even- and odd-mode characteristic impedances Z_{0en} and $Z_{0on} (n = 1, 2, \ldots, N-1)$ of the coupled line sections by using the formulae in [9], and then all the dimensions of the N coupled line sections in the proposed filtering antenna can be determined.

IV. Design Examples and Experimental Verification

In this section, an example of the proposed filtering antenna is to be presented. Following the above design procedures, a third-order Chebyshev bandpass filter with a 0.1 dB equal-ripple response, $f_0 = 2.45$ GHz, $\Delta = 14\%$, and $Z_0 = 50\ \Omega$ are firstly chosen. Based on these requirements, the inverter constants $J_{\rm n} Z_0 ({\rm n} = 1 \sim 4)$ of the bandpass filter can be calculated. Also, these parallel resonators in Fig. 4(d) have the values of $(L_{\rm n}, C_{\rm n}) = (2.068\ {\rm nH}, 2.041\ {\rm pF})$, where ${\rm n} = 1$, 2, and 3. Then, with a strip width $w = 1.17$ mm, the quality factor $Q_{\rm A} = 7.37$ is obtained by using (9). This corresponds to a strip length $l_1 = 10$ mm from the $Q_{\rm A}$-to-l_1 relationship shown in Fig. 2. To this point, all the dimensions of the inverted-L antenna are gotten, that is, $l_1 = 10$ mm, $l_2 = 17.25$ mm, and $w = 1.17$ mm. Hence, the radiation resistance $R_{\rm A}$ can be found as 28.6 Ω via Fig. 2.

Following, the inverter constant $J'_3 Z_0$ of the third coupled line and thus the even- and odd-mode characteristic impedances $Z'_{\rm 0e3}$ and $Z'_{\rm 0o3}$ can be calculated by using (10) and (4), respectively, from which the line width and the gap between lines of the third coupled line are obtained. Note that these dimensions are dependent on the characteristic impedance $Z_{\rm a}$ used in the synthesis of the filtering antenna. Fig. 6 depicts their variations as functions of $Z_{\rm a}$. It is seen that the larger is the impedance $Z_{\rm a}$, the smaller the gap size is. When $Z_{\rm a} > 50\ \Omega$, the gap would become smaller than 0.1 mm, which is difficult to realize. Thus, for easy fabrication, a characteristic impedance of $Z_{\rm a} = 30\ \Omega$ is selected here. This would correspond to an inverter constant $J'_3 Z_0 = 0.5515$ and even- and odd-mode characteristic impedances $(Z'_{\rm 0e3}, Z'_{\rm 0o3}) = (75.67\ \Omega, 42.58\ \Omega)$. Finally, the even- and odd-mode characteristic impedance of the first and second coupled line sections are calculated, and then all dimensions of each coupled line section for the proposed filtering antenna can be obtained. It should be noted that the gap size of the first coupled line section is extremely small and difficult to fabricate. To tackle this problem, the tapped structure with a

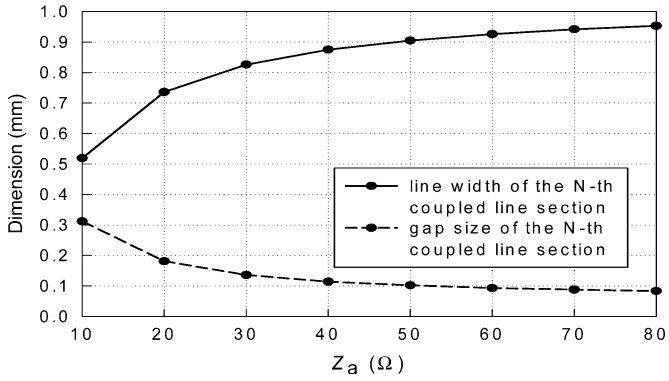

Fig. 6. Dimensions of the third coupled line section for different Z_a in the proposed filtering antenna.

quarter-wavelength impedance transformer [10] is utilized, as shown in Fig. 1(a).

The full-wave simulated return loss of the proposed filtering antenna in comparison with that of the conventional third-order Chebyshev bandpass filter is shown in Fig. 7(a). The simulated return loss of a second-order bandpass filter directly cascaded with a 50-Ω inverted-L antenna is also shown for reference. It is noticed that both of the proposed filtering antenna and filter directly cascaded with an antenna are third-order circuit, with two orders provided by the circuit and one by the antenna. These two structures occupy about the same circuit area. Here, the conventional third-order Chebyshev bandpass filter has the same specifications as the filtering antenna (14% bandwidth and 0.1 dB equal-ripple response). And the filter in the reference structure is a second-order Chebyshev bandpass filter with the same bandwidth and ripple level. It is observed that the bandwidth and skirt selectivity for the proposed filtering antenna agree very well with the conventional third-order Chebyshev bandpass filter, which demonstrates the design validity of the filtering antenna. On the other hand, putting an individually designed antenna after the bandpass filter via a simple cascaded 50 microstrip line, not only have no contribution to the order of the filter, but also deteriorate the original filter performance, especially resulting in bad skirt selectivity at the band edges.

Fig. 7(b) compares the measured return losses of the proposed filtering antenna and the conventional third-order Chebyshev bandpass filter. The simulated return loss of the filtering antenna is also shown for comparison. Likely because of the deviations in dielectric constant and substrate thickness, the bandwidth of the measured return loss of the proposed filtering antenna is slightly narrower than the simulated one. However, it is in close agreement with the measured one of the conventional third-order Chebyshev bandpass filter. Both have the same passband poles' positions, the selectivity at the band edge, and the return-loss behavior at the stopband. This demonstrates that the proposed filtering antenna has good selectivity in accordance with the conventional bandpass filter.

Fig. 8(a) shows the full-wave simulated total radiated powers of the proposed filtering antenna and the reference structure of a 2nd -order filter directly cascaded with antenna. Here, the total radiated power has been normalized to the input power. The simulated insertion loss of the conventional third-order Chebyshev bandpass filter is also shown for comparison. As compared to the reference structure, the total radiated power of the proposed filtering antenna is flat in the passband and the bandwidth is very close to the insertion-loss bandwidth of the third-order Chebyshev bandpass filter. The measured total radiated power of the proposed structure, which is in close agreement with the simulated one expect for the deviations of the bandwidth, is also shown in Fig. 8(a).

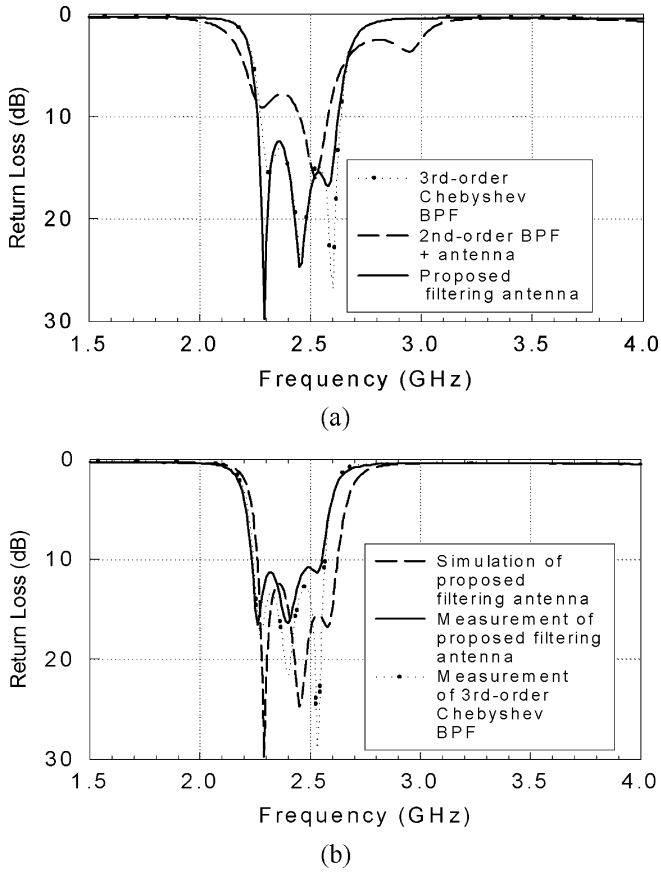

Fig. 7. (a) Full-wave simulated return losses of the proposed filtering antenna, 2nd-order r BPF + antenna, and the conventional 3rd-order Chebyshev BPF. (b) Measured return loss of the proposed filtering antenna compared with the measured one of the conventional 3rd-order Chebyshev BPF.

Fig. 8(b) shows the full-wave simulated antenna gains in the $+z$ direction versus frequency for the proposed filtering antenna and the reference structure of a 2nd -order filter directly cascaded with antenna. The simulated insertion loss of the conventional third-order Chebyshev bandpass filter is also shown for comparison. Since the inverted-L antenna has an omni-directional field pattern in the *xz*-plane, has only the antenna gain in the $+z$ direction is discussed. As compared to the reference structure, the antenna gain of the proposed filtering antenna is flat in the passband and the bandwidth is very close to the insertion-loss bandwidth of the third-order Chebyshev bandpass filter. The proposed filtering antenna also provides better skirt selectivity with stopband suppression better than 22 dB. The measured antenna gains for the proposed filtering antenna is also depicted in Fig. 8(b), which shows an antenna gain, including the circuitry loss, of -1.3 dBi. It is obvious that the measurement matches well to the simulation. The amplitude noise of the measured gain in the stopbands is due to the system noise of the antenna chamber.

In Fig. 8(b), a radiation null at $f = 2.15$ GHz in the $+z$ direction, which makes the skirt selectivity better than that of the conventional bandpass filter, has been observed. Since an inverted-L antenna alone should exhibit a monotonous gain dropping, but not a local gain minimum when the operating frequency moves away from the antenna's resonant frequency. Also, since it has been found that the frequency locations of these nulls depend on the observation angle, they are not caused by the circuit coupling between the first resonator and the third one (i.e., the inverted-L antenna) of the filter. It is finally found out that

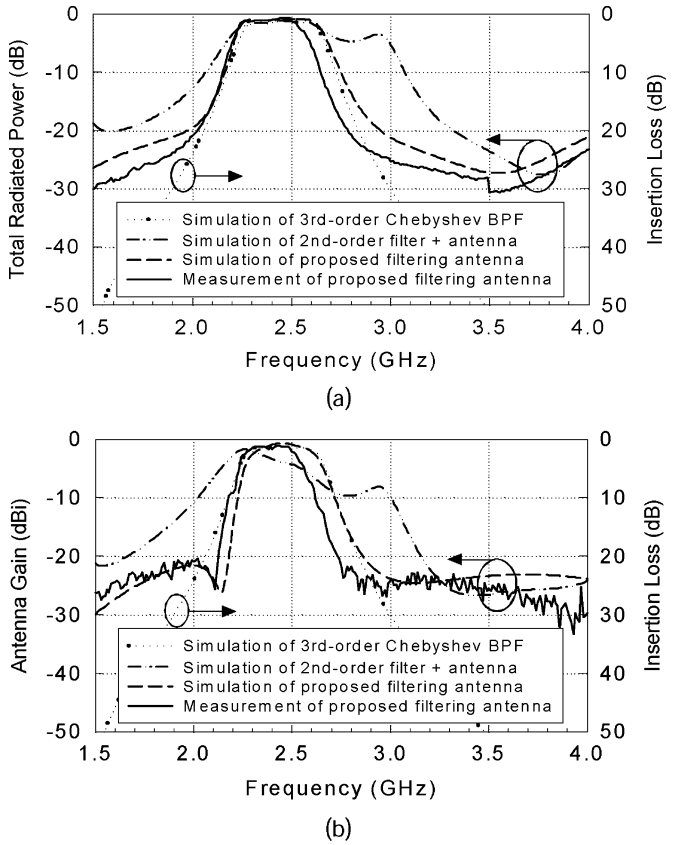

Fig. 8. (a) Full-wave simulated and measured total radiated power compared with the simulated insertion loss of the conventional 3rd-order Chebyshev BPF. (b) Simulated and measured antenna gains versus frequency in the $+z$ direction compared with the simulated insertion loss of the conventional 3rd-order Chebyshev BPF.

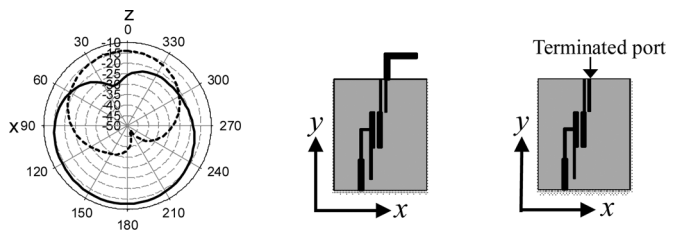

Fig. 9. Full-wave simulated total-field radiation patterns in the *xz* plane at $f = 2.15$ GHz for the proposed filtering antenna and a two-port circuit structure obtained from the filtering antenna with the inverted-L section replaced by a terminated port. [solid line: proposed filtering antenna; dashed line: two-port circuit structure.]

the last coupled line structure near the ground edge of the proposed filtering antenna induces a strong spurious ground edge current, which in turn produces extra radiation and cancels the radiation field from the antenna at some frequency. Fig. 9 shows the simulated radiation patterns in the *xz*-plane at $f = 2.15$ GHz for the proposed filtering antenna and a two-port circuit structure obtained from the filtering antenna with the inverted-L section replaced by a terminated port. It is seen that the two-port circuit produces a spurious radiation toward $+z$ direction with peak gain about -14 dBi, which is the same level as the omni-directional field pattern of an inverted-L antenna after the attenuation of the third-order bandpass filter at $f = 2.15$ GHz. For field canceling, the total radiation pattern of the filtering antenna thus possesses a radiation null near the $+z$ direction.

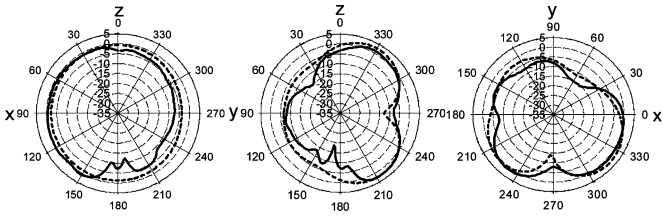

Fig. 10. Measured and simulated total-field radiation patterns in the *xz*, *yz*, and *xy* planes for the proposed filtering antenna. [solid line: measured results; dashed line: full-wave simulated results]. $f_0 = 2.45$ GHz.

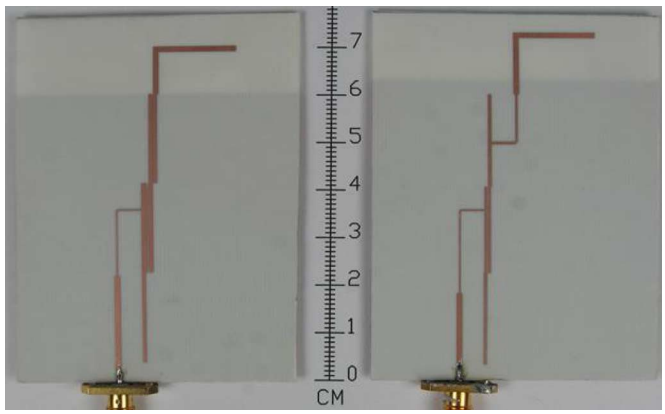

Fig. 11. Photographs of the proposed filtering antenna (left-side) and 2nd-order BPF + antenna (right-side).

The measured and simulated total-field radiation patterns at $f_0 = 2.45$ GHz in the three principal planes are also presented in Fig. 10. It is seen that the measured patterns are similar to the simulated ones, although a discrepancy occurs at $\theta = 180^\circ$ in the *yz*- and *xz*-planes (that is, the $-z$ direction) due to the interference of the feeding coaxial cable in the measurement. The radiation pattern in the *xz*-plane is nearly omnidirectional with peak gain of 0.65 dBi. Fig. 11 shows the photographs of the proposed filtering antenna compared with a second-order bandpass filter directly cascaded with an inverted-L antenna.

V. Conclusion

A filtering antenna with new co-design approach has been proposed and implemented. The design is accomplished by first extracting the circuit model of the antenna, then casting it into the synthesis of a typical parallel coupled line filter. To increase the fabrication tolerance, a quarter-wave admittance inverter with characteristic impedance other than Z_0 is introduced in the filter synthesis. A design example which has the same specifications as the conventional third-order Chebyshev bandpass filter is demonstrated. The measured results agree quite well with the simulated ones. The proposed filtering antenna provides good skirt selectivity as the conventional bandpass filter. It also possesses flat antenna gain in the passband and high suppression in the stopband.

References

[1] H. An, B. K. J. C. Nauwelaers, and A. R. V. D. Capelle, "Broadband microstrip antenna design with the simplified real frequency technique," *IEEE Trans. Antennas Propag.*, vol. 42, no. 2, pp. 129–136, Feb. 1994.

[2] B. Froppier, Y. Mahe, E. M. Cruz, and S. Toutain, "Integration of a filtering function in an electromagnetic horn," in *Proc. 33th Eur. Microw. Conf.*, 2003, pp. 939–942.

[3] F. Queudet, B. Froppier, Y. Mahe, and S. Toutain, "Study of a leaky waveguide for the design of filtering antennas," in *Proc. 33th Eur. Microw. Conf.*, 2003, pp. 943–946.

[4] F. Queudet, I. Pele, B. Froppier, Y. Mahe, and S. Toutain, "Integration of pass-band filters in patch antennas," in *Proc. 32th Eur. Microw. Conf.*, 2002, pp. 685–688.

[5] N. Yang, C. Caloz, and K. Wu, "Co-designed CPS UWB filter-antenna system," in *Proc. IEEE AP-S Int. Symp.*, Jun. 2007, pp. 1433–1436.
[6] T. L. Nadan, J. P. Coupez, S. Toutain, and C. Person, "Optimization and miniaturization of a filter/antenna multi-function module using a composite ceramic-foam substrate," in *IEEE MTT-S Int. Microw. Symp. Dig.*, Jun. 1999, pp. 219–222.
[7] A. Abbaspour-Tamijani, J. Rizk, and G. Rebeiz, "Integration of filters and microstrip antennas," in *Proc. IEEE AP-S Int. Symp.*, Jun. 2002, pp. 874–877.
[8] W. L. Stutzman and G. A. Thiele, *Antenna Theory and Design*. New York: Wiley, 1998.
[9] D. M. Pozar, *Microwave Engineering*, 3rd ed. New York: Wiley, 2005, ch. 8.
[10] M. Matsuo, H. Yabuki, and M. Makimoto, "The design of a half-wavelength resonator BPF with attenuation poles at desired frequencies," in *IEEE MTT-S Int. Microw. Symp. Dig.*, 2000, pp. 1181–1184.

Shaping Axis-Symmetric Dual-Reflector Antennas by Combining Conic Sections

Fernando J. S. Moreira and José R. Bergmann

***Abstract*—A simple procedure for the shaping of axis-symmetric dual-reflector antennas is described. The shaping procedure is based on the consecutive concatenation of local conic sections suited to provide, under geometrical optics (GO) principles, an aperture field with uniform phase, together with a prescribed amplitude distribution. The procedure has fast numerical convergence and is valid for any circularly symmetric dual-reflector configuration. To illustrate the procedure two representative configurations are investigated. The GO shaping results are validated using accurate method-of-moments analysis.**

***Index Terms*—Geometrical optics, reflector antennas, reflector shaping.**

I. Introduction

A procedure for the geometrical optics (GO) shaping of circularly symmetric Cassegrain and Gregorian antennas has been presented recently [1]. It is based on the combination of local dual-reflector systems to describe the generatrices of the sub- and main-reflectors, providing an aperture illumination with a uniform phase distribution together with a prescribed amplitude distribution. The procedure represents an improvement over traditional methods [2], [3] as no ordinary differential equation needs to be solved. The use of curved (biparabolic) surfaces to locally represent the reflectors together with ray tracing (i.e., GO concepts) had already been adopted in [4] to establish a nondifferential set of equations to shape offset dual-reflector antennas.

In [1] the authors adopted rectangular coordinates to describe the local conic sections representing the reflectors' generatrices, leading to a nonlinear algebraic equation, which was approximated to provide an one-step iterative solution. In the present work we improve the solution by using polar coordinates to represent the conic sections. That renders an one-step iterative procedure with simple linear algebraic equations, thus avoiding any approximation. Another interesting feature of the present formulation is that it is valid for any shaped axis-symmetric dual-reflector configuration based on the classical axis-displaced Cassegrain (ADC), Gregorian (ADG), ellipse (ADE), or hyperbola (ADH) [5].

Manuscript received March 25, 2010; revised July 07, 2010; accepted September 09, 2010. Date of publication December 30, 2010; date of current version March 02, 2011. This work was supported in part by the Brazilian agencies CNPq (INCT CSF), and CAPES under Grant RH-TVD-254/2008.

F. J. S. Moreira is with the Department of Electronics Engineering of the Federal University of Minas Gerais, 30161-970 Belo Horizonte, MG, Brazil (e-mail: fernandomoreira@ufmg.br).

J. R. Bergmann is with the Center for Telecommunications Studies of the Catholic University, 22453-900 Rio de Janeiro, RJ, Brazil.

Digital Object Identifier 10.1109/TAP.2010.2103028

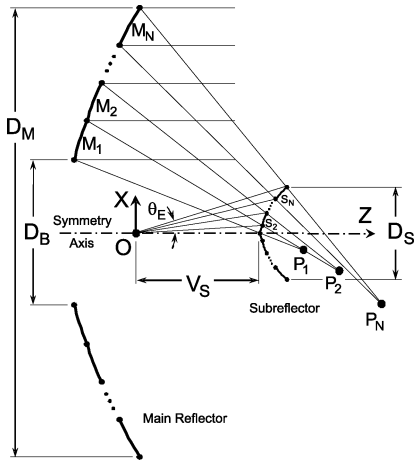

Fig. 1. Dual-reflector shaping by consecutively combining conic sections (ADC-like configuration).

In Section II the GO dual-reflector shaping formulation is presented assuming a shaped Cassegrain (or ADC) geometry. In Section III, the formulation is extended to other axis-symmetric dual-reflector configurations (ADG, ADE, and ADH). Then, the shaping of two representative dual-reflector antennas (ADC and ADE configurations) is conducted to illustrate the procedure. The convergence of the shaping procedure is investigated and compared to another procedure based on the numerical solution of an ordinary differential equation [3]. The radiation characteristics of the shaped dual-reflector antennas are numerically obtained by a method-of-moments (MoM) analysis in order to validate the applicability of the proposed shaping technique. The MoM software used in the present analysis has been successfully applied in previous reflector-antenna synthesis (e.g., [6]).

II. Formulation of the Shaping Procedure

The basic idea is to represent the reflector generatrices by conic sections consecutively concatenated, as depicted in Fig. 1. Notice that a shaped ADC configuration will be adopted to derive the formulation, but in Section III the procedure will be extended to the other axis-symmetric dual-reflector antennas [5], [7].

The conic sections describing the subreflector $(S_n, n = 1, \ldots, N)$ have two focci. One is always at the origin O (where the feed phase-center is assumed to be) and the other at point P_n. As n is varied from 1 to N, P_n spans the locus of the subreflector caustic. P_n is also the focus of the parabolic section M_n that describes a corresponding portion of the main reflector. The axis of M_n passes through P_n and is parallel to the symmetry axis of both reflectors (z axis), such that all the rays reflected at the main reflector arrive parallel to each other at the antenna aperture plane, thus providing a uniform phase distribution at the aperture, according to GO principles. Another GO principle used to define the conic sections is the energy conservation in the bundle of rays that departs from O and reflects at S_n and M_n before reaching the antenna aperture.

In order to uniquely define the conic sections S_n and M_n at each iteration n, four parameters must be determined: the focal distance F_n